THE ROYAL SOCIETY

X-ray topographic study of striation formation in layer growth of crystals from solutions

By I. L. Smolsky[1]†, A. E. Voloshin[1], N. P. Zaitseva[2], E. B. Rudneva[1] and H. Klapper[3]

[1]*Shubnikov Institute of Crystallography, Russian Academy of Sciences, 59 Leninskii Prospect, Moscow 117333, Russia.*
[2]*Lawrence Livermore National Laboratory, 7000 East Avenue, Livermore, CA 94551, USA*
[3]*Mineralogisch-Petrologisches Institut und Museum der Universität Bonn, Poppelsdorfer Schloss, 53115 Bonn, Germany*

The Lang X-ray topography method and double-crystal plane-wave X-ray topography combined with image treatment have been used to study the zonal inhomogeneity formation during crystal growth from solutions. It is shown that striation formation in crystals can be caused not only by the variations of the external growth conditions, but also by the action of some 'internal' factors such as the variations in the dislocation structure of the crystal and modification of the growth-step distribution on the growing faces. The homogeneity of rapidly grown KDP crystals (10–16 mm d^{-1}) was quantitatively evaluated with accuracy of *ca.* 10^{-7} Å.

Keywords: striation; growth steps; rapid crystal growth; lattice parameter variation; X-ray topography

1. Introduction

Conventional widespread concepts of striation formation are associated with a non-uniform impurity distribution normal to the crystallization front, which is caused by fluctuations of growth conditions (supersaturation σ, growth temperature T, etc.) (Chernov 1984). These concepts take into account possible variations in the growth rate of a face as a whole and in most cases ignore face morphology and the real structure of the crystal.

The laser-interference methods developed for studying the face morphology of crystals growing from solutions and their growth kinetics (Chernov *et al.* 1986*a*, 1987, 1988; Rashkovich 1991) have allowed observation of *in situ* crystal growth via formation of vicinal hillocks on dislocations. The hillocks are formed by growth steps and usually cover either a considerable part of the growing face of the crystal or the whole face. It was shown qualitatively in Smolsky *et al.* (1984, 1985) by X-ray topography methods that the lattice parameters of a crystal growing due to step propagation along the vicinal surface are different on different vicinal faces of the same hillocks and seem to be dependent on the growth-step orientation. This kind of

† Present address: Lawrence Livermore National Laboratory, 7000 East Avenue, Livermore, CA 94551, USA.

© 1999 The Royal Society

inhomogeneity was named 'vicinal sectorality', just as the sectoral structure of crystals is formed by growth of whole faces. The non-uniform stoichiometric composition or incorporation of impurities into various vicinal sectors on the crystal faces results in different average values of the crystal lattice parameters, which can be revealed and measured by various physical methods. As was shown in Smolsky *et al.* (1984, 1985), one of the methods suitable for crystal non-uniformity characterization, and the most sensitive to slightest distortions of the crystal lattice, is X-ray topography.

The methods of X-ray topography allow us to reveal and measure, in fact, the averaged values of crystal inhomogeneities with spatial resolution of a few micrometres. But, nevertheless, owing to the high sensitivity to the crystal lattice distortions, one can reveal some mechanisms of inhomogeneity formation in crystals during their growth from solutions if one takes into account real growth conditions of crystals which are under investigation.

2. Experimental

The study was performed on the KDP (KH_2PO_4), DKDP (KD_2PO_4) and urea ($(NH_2)_2CO$) crystals as model materials. The crystals were grown in crystallizers, 5–20 l in size, by the technique of lowering of the growth temperature. During the growth process, a square platform with a seed in the centre was alternately rotated around the vertical z-axis and thus stirred the solution. The rotation period ranged from 10 s to 1 min. In different experiments the temperature in the crystallizers was maintained with an accuracy of 0.02–0.1 °C. Once the growing crystal attained the desired dimensions, the solution was poured out and the crystal was cooled to room temperature. The specimens for further studies were cut out from the crystals.

The inhomogeneities in the crystals were revealed and qualitatively estimated using X-ray topography. We studied the 1–1.5 mm plates cut parallel and normal to the prism and pyramid faces of the crystals by the Lang (1959) method in a way similar to that described elsewhere (Smolsky *et al.* 1985; Smolsky & Zaitseva 1995). A set of X-ray topographs obtained from various specimens cut out from the same crystal allows one to draw conclusions on the distributions of inhomogeneities and defects in the crystal bulk. The topographs were exposed on the photoplates for nuclear research R-2 with a 50 μm emulsion layer. The topographic resolution was usually 5–10 μm.

Quantitatively, inhomogeneities in specimens were studied by a specially developed method that combined double-crystal plane-wave X-ray topography in the Bragg geometry with the subsequent densitometric processing of topographs. The theoretical foundations of this technique are considered elsewhere (Voloshin & Smolsky 1996*a*, *b*). In general, using this technique and a set of four experimental plane-wave topographs, we managed to determine three distortion-tensor components: the normal strain along the surface normal of the specimen, $\varepsilon^{\mathrm{T}}_{yy} = \partial u_y/\partial y$; and the components of small rotations about two mutually perpendicular axes parallel to the specimen surface,

$$w^{\mathrm{T}}_{yx} = \frac{\partial u_y}{\partial x} \quad \text{and} \quad w^{\mathrm{T}}_{yz} = \frac{\partial u_y}{\partial z}.$$

For KDP-group crystals, the above distortion-tensor components could be calculated from two topographs obtained at the angles $\varphi = 0°$ and $\varphi = 180°$, respectively (the rotation about the surface normal).

For the double-crystal reflection geometry used in our study we have

$$\left.\begin{aligned} \mathrm{d}\Theta_0 &= -w_{xx}^{\mathrm{T}} \tan(\Theta) + w_{xy}^{\mathrm{T}}, \\ \mathrm{d}\Theta_{180} &= -w_{xx}^{\mathrm{T}} \tan(\Theta) - w_{xy}^{\mathrm{T}}, \end{aligned}\right\} \tag{2.1}$$

where $\mathrm{d}\Theta_0$ and $\mathrm{d}\Theta_{180}$ are the angular deviations of the reflection maximum at the given point on the crystal surface from the average Bragg angle Θ for the crystal, and w_{xx}^{T} and w_{xy}^{T} are the distortion-tensor components.

It follows from (2.1) that

$$\left.\begin{aligned} w_{xx} &= -\frac{(\mathrm{d}\Theta_0 + \mathrm{d}\Theta_{180})}{2\cot(\Theta)}, \\ w_{xy} &= \tfrac{1}{2}(\mathrm{d}\Theta_0 - \mathrm{d}\Theta_{180}). \end{aligned}\right\} \tag{2.2}$$

To evaluate the changes $\mathrm{d}a$ in the lattice parameter, one has to take into account the dependences

$$w_{xx}^0 = \frac{\partial u_x}{\partial x} = \frac{\mathrm{d}a}{a}, \tag{2.3}$$

$$w_{xx}^{\mathrm{T}} = F^{-1}(F(w_{xx}^0) H_{22}(y, d, \omega)), \tag{2.4}$$

where F and F^{-1} are the direct and inverse Fourier transforms and $H_{22}(y, d, \omega)$ is the transfer function (Hartwig 1981; Hartwig & Lerche 1988).

The changes in the lattice parameters were measured under the assumptions that the characteristic dimension of inhomogeneities in the crystal exceeds 100 μm laterally and that the penetration depth of X-rays into the crystal does not exceed 20 μm:

$$\frac{\mathrm{d}a}{a} \approx F^{-1}\left(\frac{F(w_{xx}^{\mathrm{T}})}{H_{22}(0, d, \omega)}\right). \tag{2.5}$$

The transfer function $H_{22}(y, d, \omega)$ depends on elastic constants of the crystal and the specimen thickness d alone. The method for calculating $H_{22}(y, d, \omega)$ is described elsewhere (Hartwig & Lerche 1988).

The topographs were obtained at a 50% level of the maximum amplitude at the large-angle slope of the rocking curve. The half-width of the rocking curve obtained in the symmetric 400 reflection of KDP was *ca.* $0.7''$. The sensitivity of the method was *ca.* 3×10^{-7} Å (which provided the observation and measurement of the d-value deviation observed with the growth bands from a certain average value in the crystal). This sensitivity was attained by stabilizing the angular position of the specimen at a level of 1.4×10^{-2} seconds of arc. The densitometric measurements were made within an accuracy of *ca.* 15%, the lattice parameters were calculated to within 5% for the striations and about 30% for the sectoral and vicinal–sectoral boundaries.

3. Formation of striations due to activity changes of step dislocation sources

(*a*) *The effect of supersaturation jumps during growth*

The growth steps on the crystal faces are usually formed at the points of dislocation outcrop or dislocation bunches. They have, in the ideal case, the same height h equal

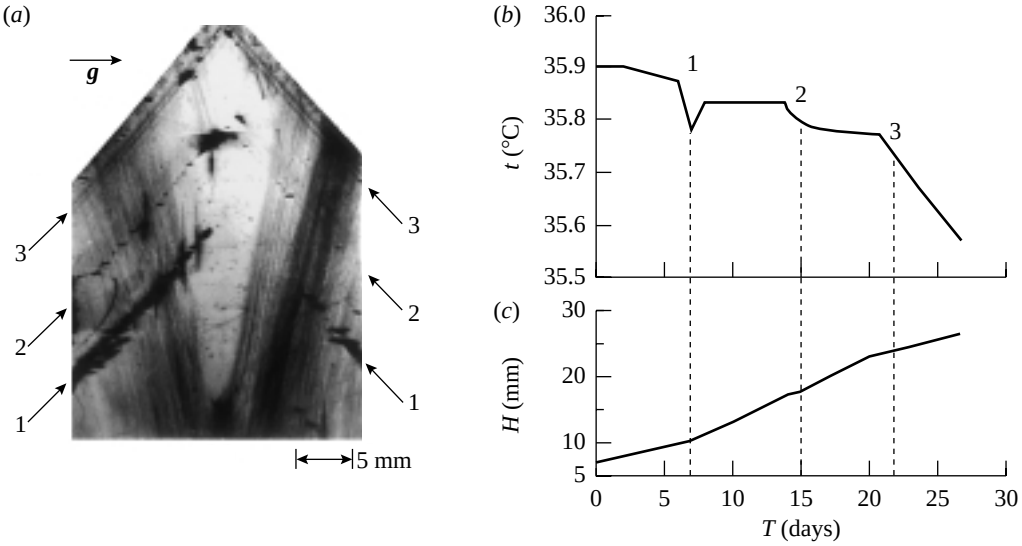

Figure 1. Striations in a urea crystal formed due to temperature jumps during growth. (*a*) Projection X-ray topograph of the (110)-cut of the crystal, Mo-$K\alpha_1$ radiation. The arrow indicates the reflection vector $\boldsymbol{g}$-[220]. (*b*) Temperature mode of the crystal growth. Numbers 1–3 indicate the moments of temperature changes. (*c*) Displacement of crystal apex during growth.

to the lattice parameter of the crystal. During the growth process, these steps form vicinal hillocks and propagate from the hillock top to the face edge with a tangential velocity v.

If a vicinal hillock is formed by a group of dislocations with the total screw component of their Burgers vectors normal to the growing face equal to mh, then, in accordance with Burton *et al.* (1951), the slope of the vicinal hillock is

$$p = \frac{mh}{(19\rho_{\mathrm{c}} + 2L)}. \tag{3.1}$$

Here $2L$ is the perimeter of the step dislocation source, ρ_{c} is the critical radius of a two-dimensional nucleus and h is the step height.

The solubility of almost all water-soluble crystalline compounds depends on the temperature (Chernov 1984). Therefore let us assume that a crystal grows for a rather long time at a constant temperature and a certain supersaturation σ_1. The long growth under steady-state conditions leads to eventual formation on each crystal face of only a few, or even only one, vicinal hillock. They are the most efficient source of growth steps with a slope $p = p_1$. This situation occurs despite the fact that the crystal usually has a considerable number of dislocations that can generate steps, although the step-generation efficiency of these dislocations is somewhat reduced, e.g. because of a reduced magnitude of the Burgers vector or a slightly lower local supersaturation above the face.

Let the supersaturation increase at a certain moment from the value σ_1 to the value σ_2 ($\sigma_2 > \sigma_1$). Beginning from this moment, new vicinal hillocks could be formed on dislocations (or dislocation bundles) characterized by a pronounced Burgers vector if the average slope of the vicinals of these new hillocks at a current supersaturation σ_2 is $p_n > p_1$. The formation of new vicinal hillocks is inevitably accompanied by the

appearance of new growth steps of various orientations that form the crystal regions having slightly different lattice parameters. They give rise to deformations that can be fixed on by the methods of X-ray topography.

Figure 1*a* shows an X-ray topograph of the (110)-cut through the centre of a urea crystal. Figure 1*b*, *c* shows the temperature variations and the growth rate of the crystal top during the growth process, respectively. One can clearly see a large number of growth dislocations and growth bands formed at moments 1, 2 and 3 due to jump-wise changes of the temperature in the crystallizer. Between these bands, one can also see similar growth bands of lower intensity. The stresses in the vicinity of growth band 1 in the crystal caused by a temperature change of 0.1 °C at moment 1 are sufficiently high to form a large number of secondary dislocation sources. The small temperature changes (0.05 °C) having occurred at moments 2 and 3 give rise to the formation of the distinct growth bands 2 and 3. They have, however, a smaller number of newly formed dislocations. Inhomogeneities of smaller scale related to smaller-temperature oscillations are seen between these growth bands. Thus, in order to grow homogeneous urea crystals without formation of new dislocations one has to stabilize the temperature during the growth process within an accuracy higher than 0.01 °C. The topographs show that the dislocation density in these urea crystals is rather high, so that there is always a sufficient number of growth-step sources. The situation is somewhat different for KDP crystals.

(*b*) *Disappearance of old and formation of new vicinal hillocks*

The distribution of growth steps over the faces of a crystal during growth is not constant. They change not only because of the variations of the external growth conditions but also because of some internal factors. We consider some of them.

Figure 2 shows an X-ray topograph of the X-cut through the centre of a KDP crystal grown at the rate $R_z \cong 10\,\mathrm{mm\,d^{-1}}$ along the Z-axis under conditions such that the anisotropy of the growth rates of the prismatic and bipyramidal faces was especially well pronounced. This anisotropy was attained by preparing a seed in such a way that its side faces coincided with the natural {100} faces. Thus, the crystal regeneration gave almost no rise to formation of dislocations that could be the powerful sources of steps on the prism faces. The orientation of growth dislocations in these crystals did not coincide with the Z-axis, and therefore they became inactive when the points of dislocation outcrop approached the face edge at a distance close to the critical-nucleus dimension $\rho_{\tilde{n}}$ and ceased generating growth steps. Then vicinal hillocks are formed on other dislocations—either already existing or newly formed. The steps generated by new dislocations have new spreading directions on the face and density in accordance with the dislocation source position and activity. Therefore some stresses between the old and new layers are formed and give rise to striation. The bands on topographs indicated by the number 3 seem to be associated with new dislocation bunches in the specimen formed, not because of the changes in the growth conditions (both temperature and supersaturation were gradually varied during crystal growth), but because the leading growth centres ceased to generate growth steps when they approached the face edges. It seems that other types of striation in this crystal are formed in the same way, but the dislocations associated with their formation are evidently outside the specimen cross-section imaged in figure 2. The dark- or light-band contrast depends on the sign change in the lattice parameter in the

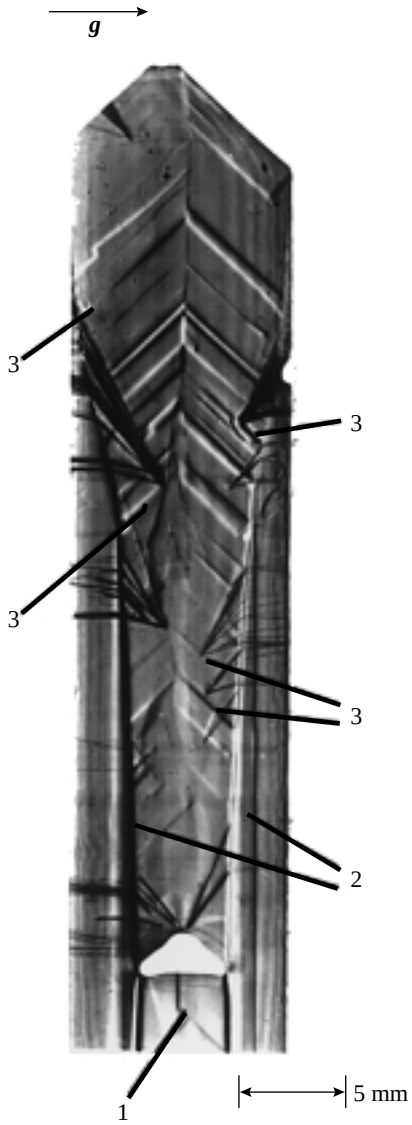

Figure 2. Projection X-ray topograph of the X-cut of a KDP crystal. Mo-$K\alpha_1$ radiation, reflection vector $\boldsymbol{g}$-[020]: (1) seed; (2) sectorial boundaries between the prismatic and bipyramidal faces; (3) striation due to a lower activity of the leading growth hillocks at the face edge and the formation of new dislocation sources of steps.

growth bands. The formation of such contrast on two-dimensional boundaries was repeatedly discussed (see, for example, Fishman & Lutsau 1970; Smolsky *et al*. 1984).

4. Growth bands caused by macrostep formation

It was found in Klapper *et al*. (1974) that dislocations in the crystals growing from solutions are oriented along directions characterized by the minimum linear energy

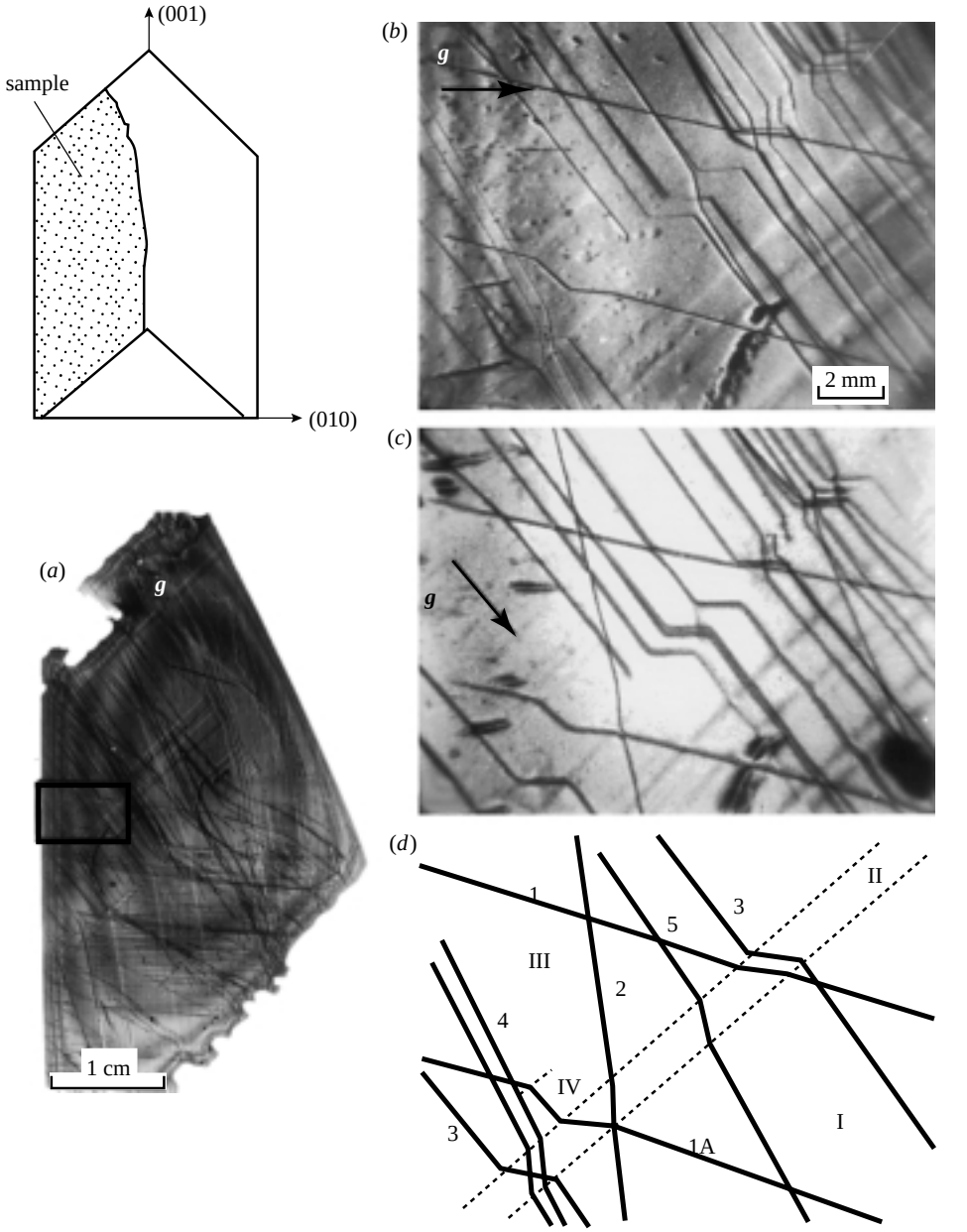

Figure 3. (*a*) Projection X-ray topograph of a part of the central cross-section of a KDP crystal (*X*-cut), $\boldsymbol{g}$-[020]. (*b*), (*c*) Topographs of the rectangular region marked on (*a*). (*b*) $\boldsymbol{g}$-[020]; (*c*): $\boldsymbol{g}$-[022]. (*d*) Schematic arrangement of dislocations in a rectangle. Numbers 1–4 indicate dislocations with different Burgers vectors.

and do not coincide with the growing-face normal. This concept was developed in a number of theoretical studies (Indenbom *et al*. 1980; Chernov & Dimitrov 1989) and was confirmed by the experiments on numerous crystals grown from solutions. However, in some instances, it was found that growth dislocations can substantially

Table 1. *Angles β formed by the dislocation line and the* [001]*-axis for dislocations with various Burgers vectors b observed and calculated in Smolsky et al. (1985) for KDP crystals grown at* 35 °C

no. (figure 3)	β (figure 1*d*) crystal region I	II	III	IV	β calculated in Klapper *et al.* (1974) (011)	(010)	Burgers vector *b* orientation
1	78	86	78		78	90	[010]
1A	78	86	78	50			
2	15	4	15		16.5	90	[001]
3	40	90	40		50	90	[110]
4	29	6	29				

deviate from these directions. On the topograph of the X-cut of the KDP crystal (figure 3*a*) almost all the dislocations originated from the regeneration zone near the seed. Most dislocation lines have kinks usually formed at the sites of the dislocation intersection with the growth bands. Similar drastic changes in dislocation orientations on growth bands were also observed in KDP, DKDP, ADP, $Ba(NO_3)_2$ and some other crystals (see Fishman 1972; Tanner & Bowen 1980). To analyse the dislocation structure, we chose a rectangular region on the topographs shown in figure 3*a–d* and determined the Burgers vectors and the angles β formed by dislocation lines and the [001]-axis for some dislocations indicated in figure 3. The data obtained are listed in table 1.

In agreement with Klapper *et al.* (1974), the orientation of growth dislocations characterized by the vector $\boldsymbol{l}$ corresponds to the direction along which the dislocation has the minimum elastic energy:

$$W = \frac{E}{\cos\alpha}, \qquad E = \frac{K\boldsymbol{b}^2 \ln(R/r_0)}{4\pi}. \tag{4.1}$$

Here E is the elastic energy per unit length of the straight dislocation, R and r_0 are the radii of the external and internal cylinders between which the linear dislocation energy is calculated, $\boldsymbol{b}$ is the magnitude of the Burgers vector, α is the angle formed by $\boldsymbol{l}$ and $\boldsymbol{n}$, and K is the energy parameter dependent on $\boldsymbol{l}$, $\boldsymbol{b}$ and the elastic constants of the crystals.

The directions characterized by the minimum elastic energy in growth sectors of the {100} and {011} prismatic and bipyramidal faces, respectively, for most widespread dislocations in KDP crystals characterized by the Burgers vectors $\boldsymbol{b}$ = [100], [001], [110], [011] and $\frac{1}{2}$[111] were determined by Fishman (1972).

The orientations of all the dislocations observed in regions I and III in figure 3*d* almost coincide with the calculated orientations (table 1), but in region II the orientations of dislocations 1, 1A, 3 and 4A drastically change, so that they nearly coincide with the optimum orientation calculated for the growth sector of the prismatic face. The orientation of dislocation 1a in region IV differs from its orientations in I–III. Lines 5 are the images of dense bunches of dislocations with various Burgers vectors (their contrast remains almost constant under various imaging conditions).

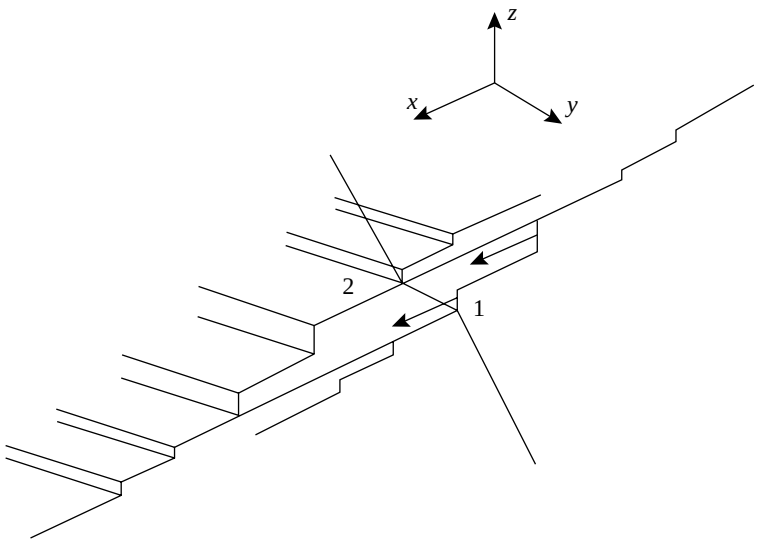

Figure 4. A model of the dislocation orientation changes in the process of macrostep formation.

It follows from (4.1) that the elastic energy per unit length in the growth direction of a dislocation depends on the direction of the Burgers vector $\boldsymbol{b}$ and the surface orientation. Since the Burgers vector of a dislocation does not change its direction during growth, the deviations observed in the experiments can be caused only by the local changes in the orientation of a growing face associated with the existence of vicinal hillocks with stepped slopes on the crystal surface.

The data on the growth kinetics obtained indicate that, at relatively low growth temperatures, these crystals show the propensity to form macrosteps, whereas at $T \approx 50\,^{\circ}\mathrm{C}$ and higher temperatures, macrosteps behave as groups of elementary steps.

If growth proceeds by the propagation of elementary steps, the orientations of growth dislocations almost coincide with the direction corresponding to the minimum dislocation energy for a singular face. In the case where elementary steps are grouped to form macrosteps or shock waves (Chernov *et al*. 1986*b*, 1988; Chernov 1992), the average surface slope at the dislocation outcrop point changes, which should result in the corresponding change of the dislocation orientation.

Let us consider that, in addition to elementary steps, a growing surface also has relatively large macrosteps, whose front can be represented as a region of the face having an orientation different from that of the remaining part. Then, at the moment of the macrostep passage through the point of the dislocation outcrop on the surface (point 1 in figure 4), the orientation of this dislocation should change in accordance with formula (4.1). Upon macrostep passage, the dislocation orientation is restored (point 2 in figure 4) if a macrostep is followed by elementary steps. This process is accompanied by the formation of two kinks, as shown, for example, in figure 3*b*, *c*. So, dislocations can indicate formation of macrosteps on the growing surface of crystal. It is clear from above that macrosteps can be a reason for the formation of striations: since the surface orientation of the macrostep front, its structure, etc., differ from those in the terraces between steps, the concentration of adsorbed impurities on

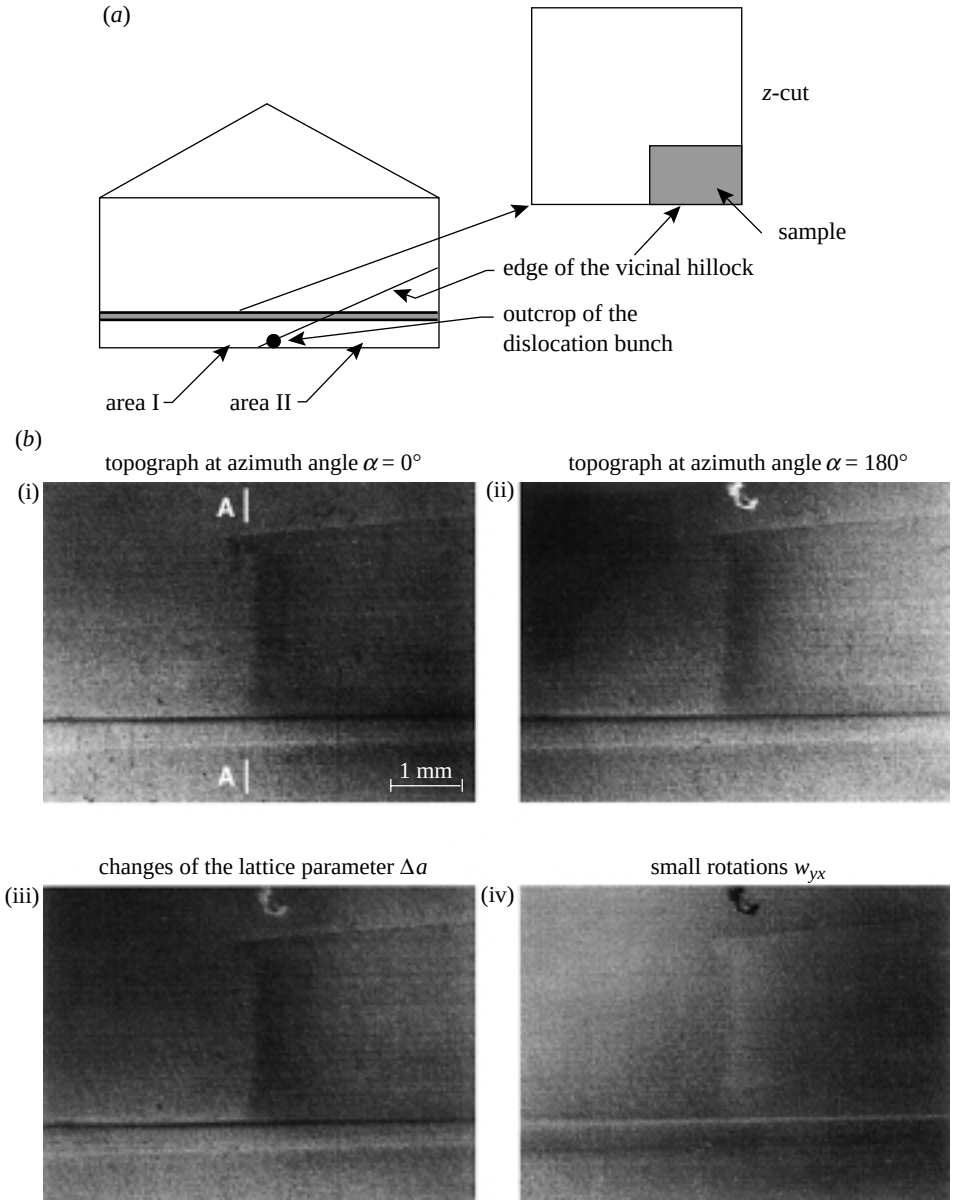

Figure 5. Striation formation in the prism sector of a DKDP crystal (growth rate $R \sim 7$ mm d^{-1} along the z-axis). (a) A diagram of a specimen position with respect to the crystal. A black spot indicates the dislocation-bunch outcrop point. (b) Plane-wave double-crystal topographs of the part of the specimen containing the vicinal–sectoral boundary (i), (ii), synthetic images of the lattice parameter changes (iii) and small rotations along the sample surface (iv).

the macrostep front should also be different. It results in the formation of X-ray topographic contrast at the edges of the region grown during macrostep passage.

A crystal plate cut from the prism sector of DKDP crystal grown with an average rate of *ca.* 7 mm d^{-1} along the z-axis is shown in figure 5. The plate was cut through

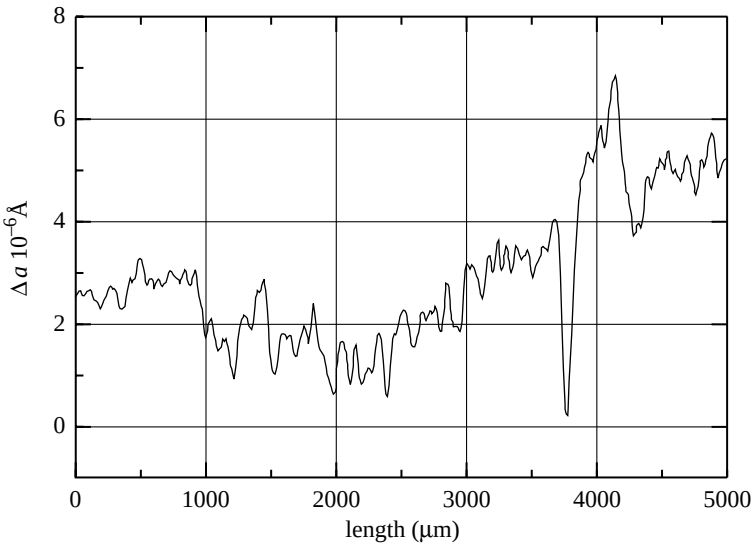

Figure 5. (*Cont.*) (*c*) The changes of the lattice parameter a along the A–A direction.

the vicinal–sectoral boundary not far from the top of the vicinal hillock marked by a black spot in figure 5*a*. The double-crystal topographs (figure 5*b*) show part of this plate with the vicinal–sectoral boundary at the central region of the images. They show a small difference in the lattice parameters between the neighboured vicinal sectors ($\Delta d \sim 5 \times 10^{-7}$). Additionally, they are rotated at an average angle of 1.2×10^{-2} arc seconds. X-ray topographs show striations formed by macrosteps during crystal growth. The variations of the lattice parameters along the A–A direction is shown in figure 5*c*. Apparently, a period of oscillations *ca.* 100 μm shows an approximate height of macrosteps because it does not correlate either with temperature oscillations in the crystallizer or with the crystal reverse rotation period.

5. Growth bands formed due to modification of vicinal hillock morphology

The nonlinear dependences of the tangential velocity v of step propagation and the slopes of vicinal hillocks on supersaturation were first established by Chernov *et al.* (1987) for KDP crystals. Figure 6 from Rashkovich (1991) shows the slope and the tangential growth rate of steps as functions of supersaturation along two directions on the prismatic face of a KDP crystal characterized by the minimum and maximum tangential growth rates, respectively (curves 1 and 2 in figure 6). It is clearly seen that with an increase of supersaturation, both slopes, p_1 and p_2, and the tangential growth rates, v_1 and v_2, drastically change at $\sigma = \sigma^* = 4.5\%$. These changes of the vicinal-hillock geometry are explained in Rashkovich (1991) by the necessity for steps to 'overcome' the blocking effect of impurities on the crystal surface.

Such changes in the morphology of a growing crystal surface result in the formation of striations visible on X-ray topographs of crystals. The projection X-ray topographs of the Z-cut of a KDP crystal grown under a varying supersaturation are shown in figure 7*c*, *d* (the corresponding variations of the supersaturation during growth is shown in figure 7*b*). One can see the boundary SA between the adjacent prismatic

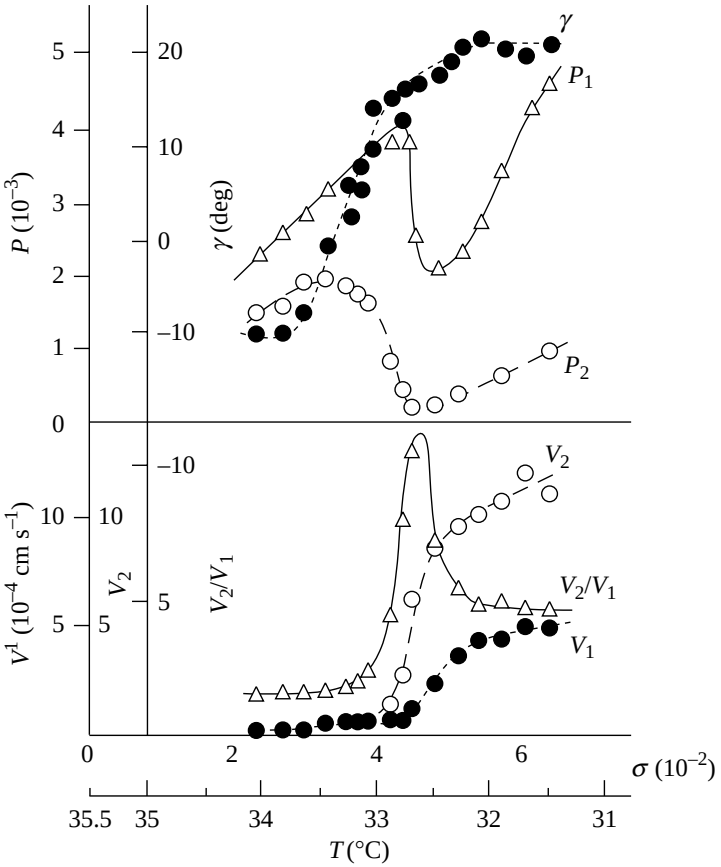

Figure 6. The slopes p_1 and p_2 and the tangential velocities v_1 and v_2 of growth step propagation along two mutually perpendicular directions of the prismatic face of a KDP crystal as functions of supersaturation; γ is the angle formed by the [100] direction and $v_{\max}$ (data from Rashkovich 1991).

and dipyramidal growth sectors and also the tilted sector boundaries SB indicated in the scheme in figure 7*a*. At first, the crystal grew rapidly on a point seed S under the supersaturation $\sigma > \sigma^*$ (figure 7*b*). Then, with a decrease in the supersaturation, the growth rate also decreased. Upon the attainment of a certain supersaturation σ^*, the morphology of vicinal hillocks on the topograph changed, which resulted in the appearance of the first growth band. At some time during which a crystal layer corresponding to growth under supersaturation $\sigma < \sigma^*$ was formed, the growth temperature was decreased at a higher rate. This increased the supersaturation again, and, at $\sigma = \sigma^*$, the second band was formed with the corresponding restoration of the vicinal-hillock morphology on the prismatic faces. This experiment allowed us to estimate the σ^* value for this crystal as 3.0–3.5%. The X-ray topographic contrast shows that lattice parameters in the band corresponding to the slow growth rate are slightly different compared with the areas of crystal grown at higher growth rates. Unfortunately, the accuracy of the growth rate and supersaturation measurements during the bulk growth is not high enough to find out the exact reason for the

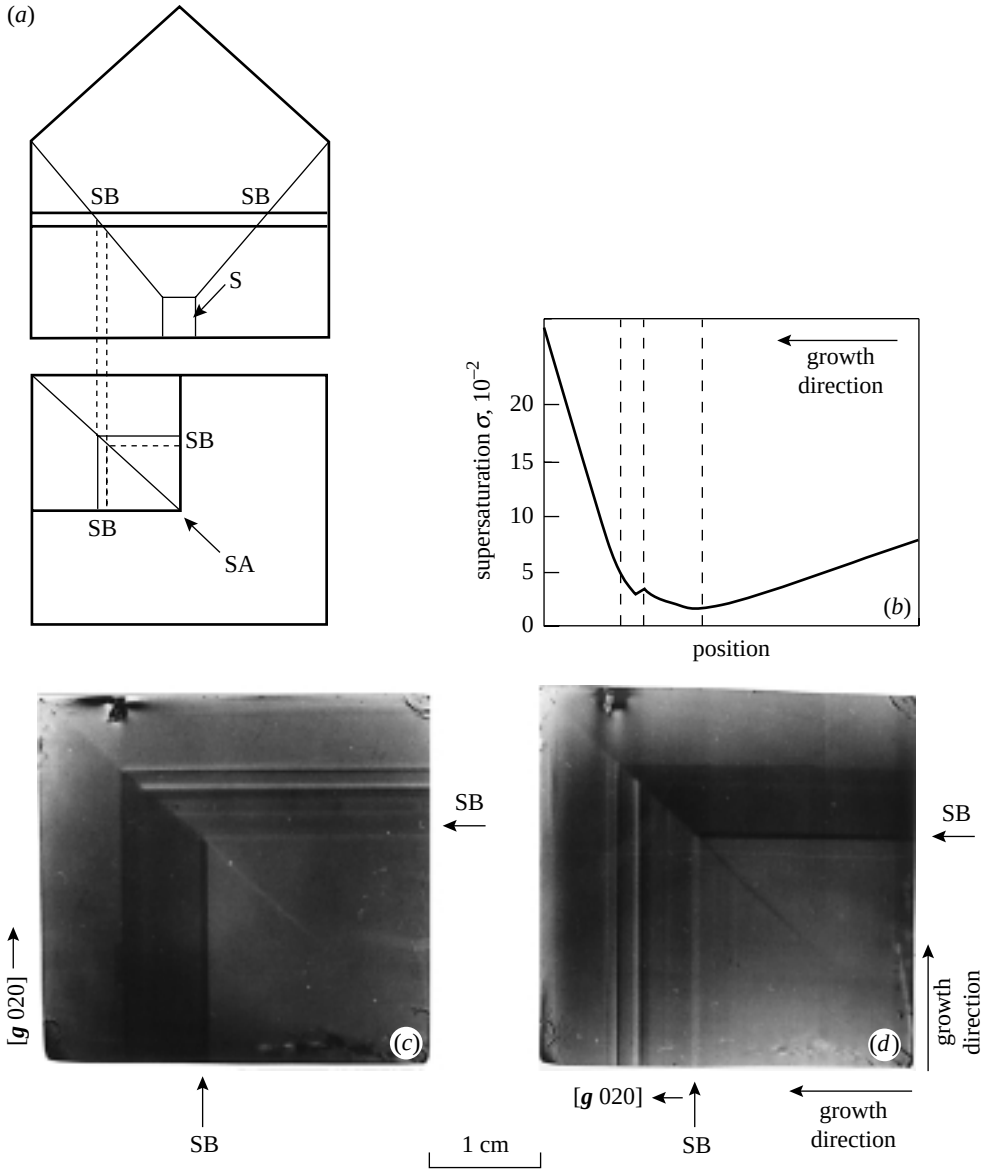

Figure 7. Formation of growth bands in the sectors of the prismatic face due to changes in the surface morphology at a supersaturation of $\sigma = \sigma^*$. (a) Scheme illustrating the orientation of the specimen with respect to the crystal and the sectoral boundaries in it; (b) the graphical representation of the changes in supersaturation during crystal growth; (c), (d) projection X-ray topographs of the Z-cut; S is the seed and SA and SB are the sectorial boundaries.

striations which are seen in the layer of the slow growth. They can be connected with variations of temperature (and supersaturation) which are typically higher in absolute value at fast growth. However, it is clear from the topographs (figure 7c, d) that the striations are much more pronounced in the area grown at $\sigma < \sigma^*$ compared with the rapidly grown area.

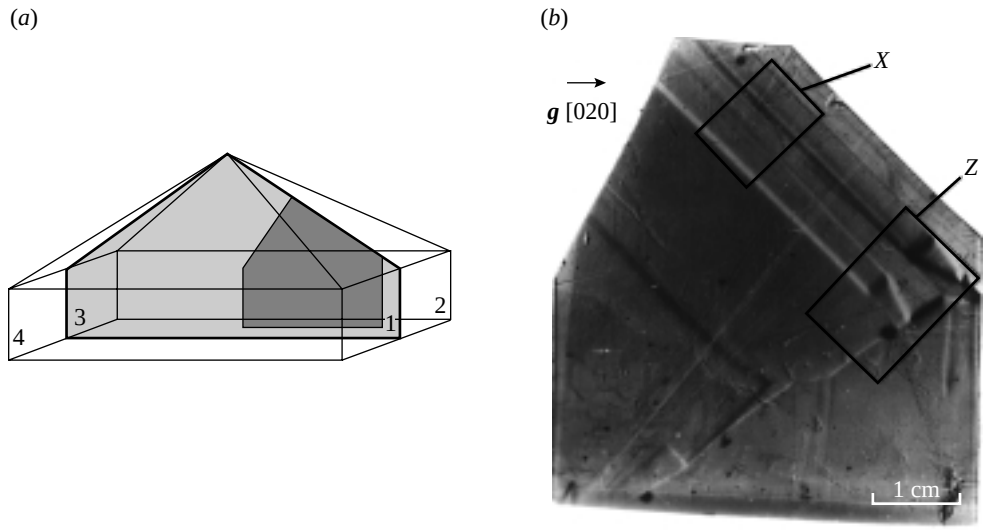

Figure 8. (*a*) Scheme illustrating the specimen position with respect to a rapidly grown KDP crystal and (*b*) the corresponding projection X-ray topograph. The quantitative measurements of striation were made in the rectangles X and Z by the methods of plane-wave X-ray topography.

Table 2. *Elastic strains in a KDP plate with normal vicinal boundaries*

area	average change in lattice parameter Δa	average value of the normal strain component ε_{yy}	average value of the ω_{yx} component of the small-rotations tensor	
	10^{-5} Å	10^{-6}	10^{-2} arc sec	10^{-7}
1	−1.6	−2.2	0.2	0.1
2	−1.6	−2.2	0.2	0.1
3	−1.0	−1.4	0.2	0.1
4	−0.5	−0.7	−1.8	−0.9
5	−0.8	−1.1	−3.4	−1.7
6	−0.4	−0.6	9.1	4.5
7	0.7	0.9	2.8	1.4
8	1.4	1.9	−4.6	−2.2
9	3.1	4.2	−2.1	−1.0

6. Homogeneity of rapidly grown KDP crystals

The methods of rapid growth ($R \cong 10$–$16\,\mathrm{mm\,d^{-1}}$) of KDP crystals (Rashkovich 1984; Akhmanov *et al*. 1984; Zaitseva *et al*. 1997) are used for synthesis of homogeneous crystals necessary for wide-aperture transformers of laser radiation. Below, we make an attempt to evaluate the level of the crystal homogeneity using the method of plane-wave X-ray topography.

The projection X-ray topograph of a certain region of the X-cut of a KDP crystal

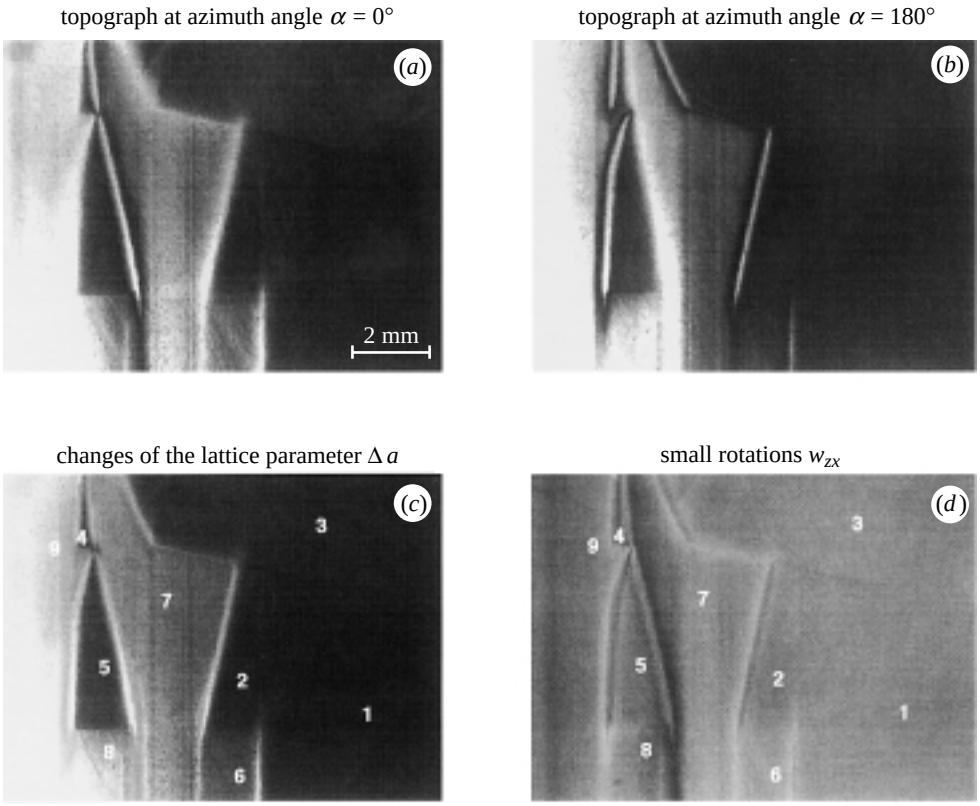

Figure 9. (*a*), (*b*) Experimental plane-wave X-ray topographs of the KDP specimen in rectangle X shown in figure 8*b*. The corresponding calculated distributions of (*c*) lattice parameter changes and (*d*) small rotations (see table 2).

grown at an average rate of 12 mm d^{-1} (24 hours) is shown in figure 8. One can clearly see striations, which, in fact, can be considered as intervicinal boundaries formed mainly as a result of the change of the leading growth centres on the dipyramidal face. The quantitative analysis of striation was performed within the rectangles X and Z shown in figure 8*b*.

The topographs of the region within the rectangle X of the *X*-cut of a KDP crystal (see figure 8*b*) are given in figure 9. The numbers denote the regions covered by the growth steps with different orientations. In this case, 1 is the growth sector of a dipyramid, 3 is the growth sector of a prism, whereas the remaining regions correspond to various vicinal sectors. In most cases the boundaries between the vicinal sectors are normal to the specimen surface, except the boundaries between sectors 5–8 and 2–6.

It should be indicated that the difference in the lattice parameters for dipyramidal and prismatic growth sectors (1 and 3) is rather small and does not exceed 6×10^{-6} Å (table 2). Therefore the contrast from the sector boundary is very weak. This is explained by the fact that the strain is maximal in the directions normal to the sectoral boundary, which makes the X-ray topography low-sensitive to such deformations in the geometry used for the topographs shown in figure 9. The exper-

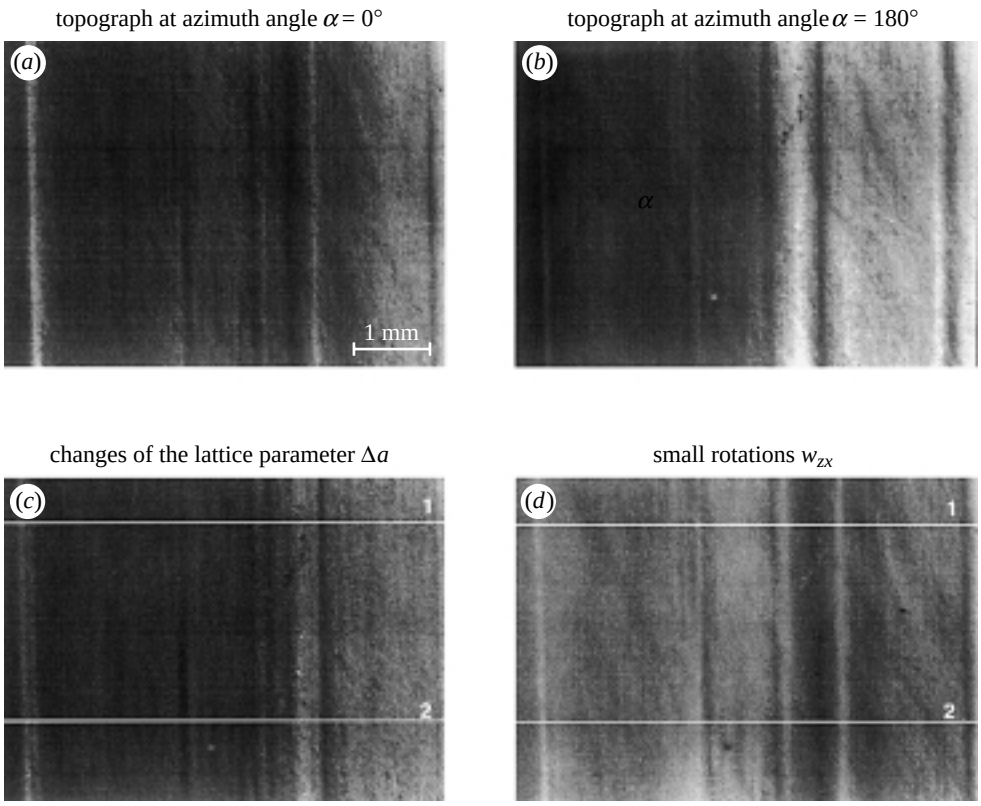

Figure 10. $(a), (b)$ Experimental plane-wave X-ray topographs of the KDP specimen in the rectangle Z shown in figure 8*b*. The corresponding calculated changes in (c) the lattice parameters and (d) small rotations.

imental plane-wave X-ray topographs of the region Z (see figure 8) are shown in figure 10a, b; the corresponding calculated distributions of the deviations of (c) the lattice parameter, Δa, and (d) small rotations are shown in figure 10c, d. These distributions measured along directions (1) and (2) are shown in graphic form in figure 11. They allow one to determine with good accuracy the deviations of the values of these quantities from their average values at any point of the region studied.

7. Conclusion

The plane-wave X-ray topography method of quantitative evaluation of crystal homogeneity has been developed. Its efficiency is demonstrated above on the example of rapidly grown KDP crystals. The method can be useful for studying the effect of various growth parameters on the crystal quality and for studying mechanisms of formation of some types of defects.

It follows from the above that formation of various inhomogeneities in crystals can be caused not only by the variations of the external growth conditions, but also by the action of some 'internal' factors, and, first of all, by the variations in the dislocation structure of the crystal. The main mechanisms of striation formation are related to redistribution of growth steps on the crystal surface, because steps with

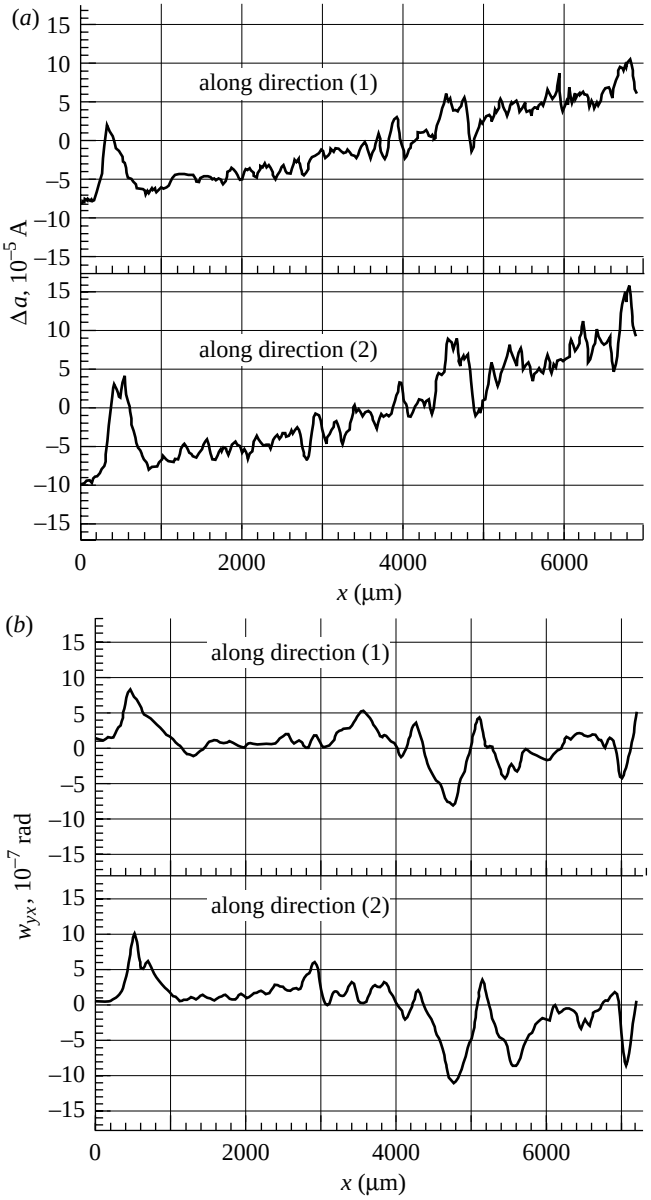

Figure 11. The distribution profiles of (*a*) the deviation of the lattice parameter along directions (1) and (2) and (*b*) small rotations along directions (1) and (2) in figure 10.

different orientations capture impurities quite differently. This results in the variation of the lattice parameter. Since there is no way known to eliminate dislocations from the crystal, there will arise vicinal hillocks formed by them and the related vicinal sectorality. The described kinds of inhomogeneity therefore have to be found in all crystals grown by layer mechanisms.

No doubt the most efficient method for growth of highly homogeneous crystals is purification of the solution prepared for crystal growth, but even in this case it

is very important to find the optimal growth conditions (e.g. supersaturation and temperature, stirring rate) to eliminate the new vicinal hillock and macrostep formations. One can also use some non-traditional methods directed to the conservation of a constant dislocation structure of the crystal during the whole growth process.

The authors acknowledge the support of the Russian Foundation of Basic Research, project no. 96-03-33316, the Lawrence Livermore National Laboratory, contract no. B304321 and the German Research Foundation, project no. 436 RUS/17/23/97.

The authors are grateful to L. Carman from LLNL and V. A. Kramarenko from IC RAN for the growth of some KDP and DKDP crystals for experiments, and also Professor A. A. Chernov and Professor L. N. Rashkovich for fruitful discussions of the results obtained.

References

Akhmanov, S. A., Begishev, I. A., Gulamov, A. A. & Rashkovich, L. N. 1984 Highly effective parametric transformation of light frequency in wide-aperture rapidly grown crystals. *Kvantovaya Elektronica* **11**, 1701–1702.

Burton, W. K., Cabrera, N. & Frank, F. C. 1951 The growth of crystals and the equilibrium structure of their surfaces. *Phil. Trans. R. Soc. Lond.* A **243**, 299–358.

Chernov, A. A. 1984 *Modern crystallography* (ed. B. K. Vainstein, A. A. Chernov & L. A. Shuvalov), 1st edn, vol. 3, ch. 1, pp. 7–232. Springer.

Chernov, A. A. 1992 How does the flow within the boundary layer influence morphological stability of a vicinal face? *J. Crystal Growth* **118**, 333–347.

Chernov, A. A. & Dimitrov, V. S. 1989 Interaction between dislocations and cellular front of crystallization: (0001) SiO_2 face. *J. Crystal Growth* **96**, 304–315.

Chernov, A. A., Rashkovich, L. N. & Mkrtchan, A. A. 1986*a* Solution growth kinetics and mechanism: prismatic face of ADP. *J. Crystal Growth* **74**, 101–112.

Chernov, A. A., Kuznetsov, Yu. G., Smolsky, I. L. & Rozhanskii, V. N. 1986*b* Hydrodynamic effects in growth of ADP crystals from aqueous solutions in the kinetics regime. *Sov. Phys. Crystallogr.* **31**, 705–709.

Chernov, A. A., Rashkovich, L. N. & Mkrtchan, A. A. 1987 Interference: optical study of surface growth processes of KDP, DKDP and ADP crystals. *Kristallografiya* **32**, 737–754.

Chernov, A. A., Rashkovich, L. N., Smolsky, I. L., Kuznetsov, Yu. G., Mkrtchan, A. A. & Malkin, A. J. 1988 Processes of crystal growth from aqueous solutions (KDP group). In *Growth of crystals* (ed. E. I. Givargizov & S. A. Grinberg), vol. 15, pp. 43–88. New York: Consultants Bureau.

Fishman, Yu. M. 1972 X-ray topographic study of the dislocations produced in potassium dihydrogen phosphate crystals by growth from solution. *Sov. Phys. Crystallogr.* **17**, 524–527.

Fishman, Yu. M. & Lutsau, V. G. 1970 X-ray dynamical diffraction contrast due to inhomogeneous impurity distribution. *Physica Status Solidi* **3**, 829–837.

Hartwig, J. 1981 Stress analysis of a crystal plate with step-like impurity distribution. *Cryst. Res. Technol.* **16**, 1297–1304.

Hartwig, J. & Lerche, V. 1988 Anisotropic deformation of a crystal plate and its analysis with X-ray diffraction method. *Physica Status Solidi* A **109**, 79–91.

Indenbom, V. L., Alshits, V. I. & Chernov, V. M. 1980 *Defects in crystals and their computer simulation*, pp. 23–37. Leningrad: Nauka.

Klapper, H., Fishman, Yu. M. & Lutsau, V. G. 1974 Elastic energy and line directions of grown-in dislocations in KDP crystals. *Physica Status Solidi* A **21**, 115–129.

Lang, A. R. 1959 The projection topography: a new method in X-ray diffraction microradiography. *Acta Crystallogr.* **12**, 249–250.

Rashkovich, L. N. 1984 High-speed growth of large crystals for nonlinear optics from solution. *Vestn. Akad. Nauk SSSR* issue 9, 15–19.

Rashkovich, L. N. 1991 *KDP-family single crystals*, 1st edn, pp. 1–202. Bristol: Adam Hilger.

Smolsky, I. L. & Zaitseva, N. P. 1995 Characteristic defects and imperfections in KDP crystals grown at high rates. In *Growth of crystals* (ed. E. I. Givargizov & S. A. Grinberg), vol. 19, pp. 173–185. New York: Plenum.

Smolsky, I. L., Chernov, A. A., Kuznetsov, Yu. G., Parvov, V. F. & Rozhanskii, V. N. 1984 Vicinal sectorality and its relation to growth kinetics of ADP crystals. *Sov. Phys. Dokl.* **29**, 703–705.

Smolsky, I. L., Chernov, A. A., Kuznetsov, Yu. G., Parvov, V. F. & Rozhanskii, V. N. 1985 Vicinal sectorality in the growth sectors of the (101) faces of ADP crystals. *Sov. Phys. Crystallogr.* **30**, 563–566.

Tanner, B. K. & Bowen, D. K. (eds) 1980 *Characterization of crystal growth defects by X-ray methods*. New York: Plenum.

Voloshin, A. E. & Smolsky, I. L. 1996*a* Determination of quasiplastic strains in a crystalline plate based on a solution of the inverse problem of the theory of elasticity (one-dimensional case). *Physica Status Solidi* B **192**, 73–86.

Voloshin, A. E. & Smolsky, I. L. 1996*b* Problems of X-ray topography analysis of one-dimensional inhomogeneities in crystals. In *Structural studies of crystals, problems of modern crystallography*, pp. 184–206. Moscow: Nauka.

Zaitseva, N. P., De Yoreo, J. J., De Haven, M. R., Vital, R. L., Montgomery, K. E., Richardson, M. & Atherton, L. J. 1997 Rapid growth of large-scale (40–55 cm) KH_2PO_4 crystals. *J. Crystal Growth* **180**, 255–262.